

UNCLASSIFIED

Q # 2174 Q121

46-56

CONTROL SYSTEMS LABORATORY

ELEMENTARY THEORY OF SHADOWING
BY A ROUGH SURFACE

Bruce L. Hicks

Report R-81

March 1956

Contract DA-36-039-SC-56695
Project 8-103A,D/A Project 3-99-10-101

Encl. *8*...to BUSHIPS ser. *855-033*

UNIVERSITY OF ILLINOIS · URBANA · ILLINOIS

RRU-134 J UNCLASSIFIED

"The research reported in this document was made possible by support extended to the University of Illinois, Control Systems Laboratory, jointly by the Department of the Army (Signal Corps and Ordnance Corps), Department of the Navy (Office of Naval Research), and the Department of the Air Force (Office of Scientific Research, Air Research and Development Command), under Signal Corps Contract DA-36-039-SC-56695, Project 8-103A, D/A Project 3-99-10-101."

Report R-81

ELEMENTARY THEORY OF SHADOWING BY A ROUGH SURFACE

March 1956

By
Bruce L. Hicks

CONTROL SYSTEMS LABORATORY
UNIVERSITY OF ILLINOIS
URBANA, ILLINOIS
Contract DA-36-039-SC-56695

Numbered Pages: 26

Elementary Theory of Shadowing by a Rough Surface

Bruce L. Hicks

	Page
ABSTRACT	1
INTRODUCTION	3
PART I - THEORY FOR LARGE GRAZING ANGLES	4
1. General Method	4
2. Assumptions	6
3. Local Shadowing	7
Definitions	7
Basic Equations	8
Properties of Specific Shape Functions	10
Extreme Cases	12
4. Statistics of Maximum Slopes	13
5. Ensemble Averages	14
6. "Lower Limit" of the Fraction Shadowed	17
7. Discussion	18
PART II - THEORY FOR SMALL GRAZING ANGLES	21
8. Development of the Theory	21
9. Discussion	25
CONCLUDING REMARKS	26

ELEMENTARY THEORY OF SHADOWING BY A ROUGH SURFACE

Bruce L. Hicks

ABSTRACT

The shadowing by idealized models of the sea or other rough surface is calculated for short wave-length radiation. For all the models studied it is found that the fraction shadowed, averaged over the surface, is a function only of the ratio (μ/σ_m) where μ is the slope of the incoming ray and σ_m is the rms wave slope.

In Part I of the paper, a theory of shadowing is developed for two models of the sea surface which it is appropriate to use when the grazing angle of the ray is large. In the first model, shadowing of a wave by the nearest crest is considered, but shadowing of that wave by more distant crests is neglected. It is also assumed that all wave crests lie at the same height, that the waves possess no fine structure, and that the ensemble of waves can be represented by a one parameter family of slope functions. The distribution function for this parameter (the maximum slope) characterizes the statistics of the first model. Except for large grazing angles we should expect that this first model would lead to calculated values of the fraction shadowed of the surface that are too small. A second model is therefore also considered which would surely give a lower bound to the fraction shadowed. This model allows no variation of slope function or of statistics.

A number of numerical calculations based on the two models are described. First, the effect of the shape of an individual wave upon its local shadowing is discussed for a variety of shape functions. A general formula is obtained for the local fraction shadowed of any

smooth-crested wave whose maximum slope slightly exceeds the slope of the incident ray. Next the calculated average fraction shadowed $\tilde{\lambda}$ for ensembles of waves is discussed for the second model, and, for two choices of wave statistics, also for the first model. For large values of (μ/σ_m) , and therefore for small values of $\tilde{\lambda}$,

$$\tilde{\lambda} \sim (\mu/\sigma_m)^p \exp[-c(\mu/\sigma_m)^q]$$

where p varies from -1 to 3 and $q = 1$ or 2 for the two models, two wave statistics, and various shape functions. For any value of (μ/σ_m) greater than about two, the value of $\tilde{\lambda}$ for the second model is found to be less than the value of $\tilde{\lambda}$ for the first model, for all shapes and statistics, as was expected. For smaller values of (μ/σ_m) this is no longer the case, possibly owing to the use of incorrect distributions of maximum slope. It is encouraging perhaps that the values of $\tilde{\lambda}$, for given values of (μ/σ_m) and two realistic shape functions, are substantially the same for the two rather different distribution functions we employed.

In Part II, a heuristic shadowing theory is developed for rays incident at very small grazing angles. The problem of calculating the shadowing is here reduced to a problem of finding the fraction of light that is transmitted through a box containing a collection of opaque obstacles. For this third model it is found that $\tilde{\lambda}$ is of the form

$$\tilde{\lambda} = 1 - \exp(-\Lambda\sigma_m/\mu)$$

where the parameter Λ may depend upon characteristics of the sea state other than the rms slope σ_m . Comparison with the second model is also profitable here, for this model should give a lower limit to the fraction shadowed $\tilde{\lambda}$ for small as well as large grazing angles. However, the third model yields values of $\tilde{\lambda}$ which are larger than the "lower limit" values of the second model only if Λ is greater than about 0.5,

which is a value that is somewhat larger than would be estimated for two of the idealized wave shapes used for the first model.

These various calculations are combined to give a rough estimate of the fraction shadowed $\tilde{\lambda}$ for all values of (μ/σ_m) in the range 0.2 to 4.0. Since σ_m is determined by the wind speed, this estimate and the calculations upon which it is based may be of some use in correlating experimental data on shadowing. A more complete theory than ours should be able to predict the dependence of shadowing not only upon the rms value of the wave slope but also upon other relevant sea state statistics.

INTRODUCTION

We are interested in the phenomenon of shadowing by a rough surface in connection with sea clutter studies because, for small enough grazing angles, the forward or back scattering of radiation is decreased by the effects of shadowing.* Oceanographers also are interested in shadowing because it influences the apparent optical brightness of the sea surface near the horizon. In this paper we shall consider the question of what areas lie in shadow but not the more difficult problem of what fraction of these areas are visible at different viewing angles.

We shall restrict our treatment of shadowing to profiles formed by the intersection of the random rough surface with vertical planes lying in azimuthal directions of interest. We shall not be concerned with the correlation between neighboring profiles whether formed by parallel or intersecting vertical planes.

*H. Goldstein, "A Primer of Sea Echo," Report 157 (1950) of the U. S. Navy Electronics Laboratory.

The geometry of shadowing is illustrated in Fig. 1 which shows one idealized wave profile formed by the intersection of a vertical plane with the rough surface. Of those rays of slope μ lying in this vertical plane, one, the limiting ray, is tangent to the profile. Its points of tangency and intersection with the profile mark the limits of the shadowed region. For each wave profile and each ray slope μ , a certain fraction of the profile lies in shadow.

It will be our object to calculate this fraction shadowed, averaged over many wave profiles which together constitute one profile of a randomly rough surface.

PART I. THEORY FOR LARGE GRAZING ANGLES

1. General Method

We visualize, as a general basis for the first model we shall use,* that the random process corresponding to the profile can be described by a hierarchy of successively more detailed representations. Each representation of the hierarchy consists of a set of approximating functions, each member function of any one set being fitted to the "resultant" wave** that lies between two crests on the rough surface. In the first set of the hierarchy, only the high crests are considered, that is the smaller scale structure of the surface is neglected. The "resultant" wave lying between each pair of high crests is then fitted by a shape function with no maxima and at most one turning point between the two high crests.

*The second model will not be introduced until Sect. 6.

**The word "resultant" emphasizes our interest in the local shape of the water surface rather than in the shape of component gravity waves of different periods whose superposition, at any instant, forms the water surface.

In the second set of functions in the hierarchy, allowance would be made for (at most) one maximum between each pair of high crests. Further details of the hierarchy are not needed for present purposes since it is only the simplest description of the surface that we employed for calculations described in this paper, and a mention of the higher members of the hierarchy is made only to permit visualization of how our elementary methods might fit into a more comprehensive treatment of shadowing for large grazing angles.

For a given order of approximation, that is for a given set in the hierarchy of representations, we consider a type of shape function that contains a certain number of parameters. The values of these parameters would then be chosen successively in such a way that the shape function fits in turn, and as well as the order of approximation allows, each wave in the ensemble of resultant waves making up the sea surface. Thus when the basic shape function has been chosen, the ensemble of resultant waves will be represented, with more or less accuracy, by the set of values assumed by the parameters. Any quantity whose value depends only on the shape of an individual resultant wave and not upon its neighbors--for example, the shadowing of a single wave, the second moment of its slope distribution, etc.--can in principle be calculated from a knowledge of the shape function and the values of the parameters designating that particular wave. The quantity is in fact a function of the parameters characterizing the different member waves of the ensemble. Ensemble averages of such quantities correspond to appropriately weighted averages over the parameters. In particular we may calculate the average fraction of a profile that is shadowed and certain measurable statistics of the wave ensemble such as the variance of the surface slope.

The shape function and the parameters can be chosen in any way that provides an appropriate local description of the profile. With such freedom of choice, it is of course necessary to fix the statistics of the parameters

by making proper use of whatever statistics are known for the representative wave ensemble, so that as little arbitrariness as possible remains in the computed value of the shadowing for the random surface.

2. Assumptions

The broad program just outlined must be narrowed somewhat in order that specific calculations can be made. We shall assume that we are interested only in back scattering and shall not consider forward scattering or off-angle scattering at all. (The back scattering case is also the easier one.)

Further assumptions are:

- (a) The wave length of the radiation is much less than the scale of the roughness so that there are no diffraction effects to be considered. This amounts in the radar case to making a sharp division between those waves which are scatterers but are too small to give geometrical shadowing, and those waves which are shadowers but are too large to produce important diffraction of the radiation. It is clear that in making this arbitrary division we shall be ignoring a class of waves which produce both shadowing and diffraction.
- (b) The earth is flat, or more specifically, the elevation of the water surface, relative to a plane of reference, and averaged over any large group of successive waves is the same, within statistical fluctuations, no matter which set of such waves is chosen from the profile.
- (c) Only the large peaks are considered, that is only one scale of crests, and the smaller ones are smoothed out, thereby restricting us to the simplest or least accurate member of the hierarchy of representations.
- (d) All of the large peaks considered are of the same height, and therefore the shadowing of each wave can be treated separately.

This assumption is clearly the most restrictive one and the one which is most important to discard in future and better calculations.

- (e) One parameter is used to characterize each individual resultant wave lying between a pair of adjacent crests. This one parameter is the maximum slope M of each resultant wave. Various forms of local shape function are, however, considered.
- (f) Two statistics of the parameter M are considered. In each case the variance of M for the assumed statistics is found in terms of a moment of the shape function and the variance of the wave slopes. The latter quantity, in our theory, characterizes the sea state.

3. Local Shadowing

Definitions. Let us consider a single wave. The horizontal distance between the two crests of the wave is taken to be the wave length L . Each of the two crests may be either sharp or smooth.

Any incident ray of slope μ relative to the plane of mean sea level creates a shadowed region if it touches the profile at two points and lies above the profile between these two points, as is illustrated in Fig. 1. One of the points (x_1, y_1) lies lower than the other and is, according to our assumptions, a point of intersection. The higher point (x_0, y_0) will be one at which the incident ray is tangent to the profile, if the nearby crest is smooth. This higher point will lie at the crest itself, for the shapes to be studied, if the crest is sharp.

We measure the shadowed length by the horizontal distance, $L_s = x_0 - x_1$, between the two points at which the incident ray touches the profile. Between these two points there will lie, for the shapes

studied, one other point (x_2, y_2) at which the slope of the profile is equal to that of the incident ray. The corresponding distance $(x_0 - x_2)$ we designate by L_* .

There are several reasons for our using the horizontal length of the wave that is shadowed as a measure of the shadowing. The slopes of a profile of interest are seldom as much as 0.3, so that there is usually little difference between the arc length that is shadowed and its horizontal projection. Furthermore, each problem involving shadowing introduces a different relationship between the slopes of the unshadowed parts of the profile and the scattering properties of the profile. When these relationships become known for each problem, then our calculation, which involves only the horizontal lengths of the shadowed and unshadowed parts of the profile, can perhaps be extended appropriately. It is clear also that our calculation will be more simple if we measure the shadowed length by its horizontal projection rather than by the shadowed length of arc along the profile.

It is convenient to use dimensionless quantities, $\xi_1 = x_1/L$ obtained by dividing the various horizontal distances by the wave length L . Then the fraction λ of a single wave that is shadowed, i.e., the fraction shadowed locally, is

$$\lambda = \xi_0 - \xi_1 = L_s/L \quad (1)$$

and the fraction corresponding to L_* is

$$\lambda_* = \xi_0 - \xi_2 = L_*/L \quad (2)$$

It is clear that $\lambda_* \leq \lambda$. The ensemble averages of λ and λ_* are denoted by $\tilde{\lambda}$ and $\tilde{\lambda}_*$.

Basic Equations. Let us suppose that the shape function used to describe a single wave is

$$y = f(x) \quad (3)$$

This can generally be reduced to the convenient dimensionless form

$$\eta = \zeta(\xi) \quad (4)$$

by the transformations

$$x = L\xi \quad (5)$$

$$y = M\eta \quad (6)$$

where M is the largest value taken by the slope $f'(x)$ of the profile at or between the two crests defining a given wave. The relation between the derivatives is then

$$f'(x) = M \zeta'(\xi) \quad (7)$$

A convenient measure of the slope μ of the incident ray is the quantity

$$v = \mu/M \quad (8)$$

since $\lambda \rightarrow 0$ when $v \rightarrow 1$ for any shape function we consider.

It is easy to show that the relationship

$$\lambda v = \eta(\xi_0) - \eta(\xi_0 - \lambda) \quad (9)$$

holds among the three quantities ξ_0 , v and λ . This equation is valid whether the crest near (ξ_0, η_0) is sharp or smooth. A second condition involving ξ_0 is needed in order that the desired relationship between λ and v alone can be expressed, at least implicitly. If, of the two high crests defining a resultant wave, the one lying closer to the source of radiation is sharp, then the needed second condition is simply that ξ_0 is the abscissa of the position of this crest. If, however, the crest lying near the source is smooth, then the second condition is

$$v = \eta'(\xi_0) \quad (10)$$

In order to find λ_* , we use the equation

$$v = \eta'(\xi_0 - \lambda_*) \quad (11)$$

to replace Eq. 9 and the same conditions as before, for the two types of crest, to eliminate ξ_0 .

Properties of Specific Shape Functions. We have chosen for study a number of shape functions which are illustrated in Fig. 2* and listed below. Other functions and properties derived from each shape function are also listed, namely, the fraction shadowed locally, λ , and the ratio (λ_*/λ) as functions of v ; the relationship between M , the maximum slope and δ , the height to length ratio of the resultant wave; and the quantity α_2 which is added for later reference. Figs. 3, 4, and 5 show the variation of λ and λ_*/λ with v .

Quadratic

$$\begin{aligned} \eta &= \xi^2 & \alpha_2 &= 1/3 \\ \lambda &= 1 - v & \delta &= M/4 \\ \lambda_*/\lambda &= (1-v)/2 \end{aligned}$$

Wilton's Cycloid**

$$\begin{aligned} \xi &= 2\delta(\theta + \sin \theta) & \delta &= (2\sqrt{3} + \frac{4\pi}{3})^{-1} \\ \eta &= 2\sqrt{3} \delta(1 - \cos \theta) & M &= 1/\sqrt{3} \\ \lambda &= 2\delta(\frac{\pi}{3} + \frac{\sqrt{3}}{2} - \theta_1 - \sin \theta_1) \\ \lambda v &= 2\sqrt{3} \delta(\cos \theta_1 - 1/2) \end{aligned}$$

*In order to permit easy comparison of the wave shapes, the origins for the several shape functions have been displaced so that the crests lie at $\xi = \pm 0.5$ for all of the wave shapes.

**Phil. Mag. 26, 1053 (1913). Each wave is a piece of a cycloid. The crest angles are 120° , corresponding to the steepest classical waves.

Cubic A

$$\begin{aligned}\eta &= \xi - 3\xi^3 & \alpha_2 &= 6/5 \\ \lambda &= (1-v)^{1/2} & \delta &= 4M/9 \\ \lambda_*/\lambda &= 2/3\end{aligned}$$

Cubic B

$$\begin{aligned}\eta &= \xi^3 - 1/3\xi & \alpha_2 &= 2/15 \\ \lambda &= 1-v^{1/2} & \delta &= 4M/27 \\ \lambda_*/\lambda &= \left[2 - (3v + 1)^{1/2} \right] / 3(1-v^{1/2})\end{aligned}$$

Cosine

$$\begin{aligned}\eta &= (1/2 \pi) \cos 2\pi\xi & \alpha_2 &= 1/2 \\ \operatorname{tg} 2\pi\xi_0 &= -(1 - \cos 2\pi\lambda) / (2\pi\lambda - \sin 2\pi\lambda) & \delta &= M/2\pi \\ v &= -\sin 2\pi\xi_0 \\ \lambda_* &= (1/\pi) \cos^{-1} v\end{aligned}$$

We note that the local shadowing, in the terms we have chosen to describe it, varies considerably with the type of shape function that has been specified. As will be seen later, the ensemble average of the fraction shadowed will give a slightly different picture because another factor, namely the ratio of rms slope to maximum slope for each shape function, also enters the calculations. We notice further, in Fig. 5, that the fraction λ_*/λ is often considerably less than one and never exceeds one, just as we would expect from the geometrical situation. We should therefore also expect that the ensemble average of λ_* , namely $\tilde{\lambda}_*$, should never exceed, for a given shape function, the ensemble average of λ , namely $\tilde{\lambda}$.

Extreme Cases. Special calculations can be made to clarify further the local situation for values of ν either near zero or near unity. When ν is small compared to unity, then each smooth crest can be represented by an inverted quadratic parabola. The resulting approximate formula for the fraction shadowed for a wave bounded by two smooth crests is:

$$\lambda \cong 1 - \left[\frac{(\mu/c_0 L)(\gamma-1)}{\gamma} \right] - (1/\gamma) \left[-(\gamma-1)(\mu/c_0 L)^2 + 2\gamma(\mu/c_0 L) \right]^{1/2} \quad (12)$$

where C_0 and γC_0 are the curvatures respectively of the crest to which the ray is tangent and the one it intersects, and L is the distance between the two (parabolic) crests. The corresponding local shadowing curves in the neighborhood of $\nu = 0$ are shown in Fig. 4 and may be compared with the corresponding parts of the shadowing curves for the various complete shape functions considered above. To make the comparison, for example, in the case of the cosine shape, we put

$$C_0 L = 2\pi M \quad (13)$$

where M refers to the maximum slope of a sinusoid that fits the right hand parabolic crest. Then for ν near zero, the λ vs. ν curves have the same curvature, for parabolic crests of equal curvature ($\gamma=1$), as do the λ vs. ν curves for the cosine shape.

When ν is nearly equal to unity, then the shape function we have designated by Cubic A can be shown always to yield a good approximation to the (small) fraction shadowed when the incident ray is tangent to the wave near a turning point. For in the neighborhood of a point x_m of maximum slope M (or turning point) of a profile we can represent the profile by the expansion

$$y = f(x) = f(x_m + \Delta) = f(x_m) + \Delta M + 1/6 \Delta^3 f^{(iii)}(x_m) + \dots \quad (14)$$

Let

$$x_0 = x_m + \Delta_0, \quad x_1 = x_m + \Delta_0 + \Delta_2 \quad (15)$$

be the points of intersection and tangency of the ray of slope μ .

Then it can be shown that

$$\Delta_2 = -3\Delta_0 + 3/2 \Delta_0^2 f^{(iv)}(x_m)/f^{(iii)}(x_m) + \dots \quad (16)$$

Neglecting the term in $f^{(iv)}(x_m)$ yields, as we would expect, the same relation as for a cubic,

$$-\Delta_2 \approx 3\Delta_0, \quad (17)$$

between the shadowed length $-\Delta_2$ and the distance Δ_0 from the inflection point to the tangent point. If $f^{(iv)}(x_m)$ and higher terms are not neglected then we can calculate corrections to the shadowed length owing to departure of the curve near $x = x_m$ from the cubic shape.

4. Statistics of Maximum Slopes*

The distribution functions for maximum slope M are assumed to be normalized in the range 0 to ∞ . The variance of M is σ_M^2 . The distribution function is then of the form

$$(1/\sigma_M) P(M/\sigma_M) \quad (18)$$

We did not find any published information on sea surfaces which would directly determine the nature of $P(M/\sigma_M)$. However, the probability is small that a given wave will have a maximum slope that is either very small or very large compared to σ_M . We choose first therefore a distribution function of exponential type

$$P(M/\sigma_M) = 6(M/\sigma_M) \exp(-6^{1/2} M/\sigma_M) \quad (19)$$

A few calculations are also discussed for the Gaussian function

$$P(M/\sigma_M) = (2/\pi)^{1/2} \exp(-M^2/2\sigma_M^2) \quad (20)$$

*The assumption of equal crest heights, for this first model, makes it unnecessary to consider the statistics of wave height. Its probability distribution would not be significant even for more advanced models, but some higher order functions such as autocorrelation functions would be relevant.

in order to discover what effect upon $\tilde{\lambda}$ such a change in statistics would produce.

Although we are considering here just the one parameter, the maximum slope M , it is clear that a more thorough statistical treatment would include other parameters such as the wave length L or possibly the distance between points of maximum slope in one profile. Since the distribution of M is assumed to be independent of that of L in our theory, ensemble averages of functions of slope, such as its moments or the fraction shadowed, will not require knowledge of the distribution of L .

5. Ensemble Averages

We are first interested in the statistics of the slopes of our wave ensemble. The symbols $\alpha_r M^r$, \mathcal{M}_r and \tilde{m}_r are used to designate the r -th moment of the slope of an individual wave, of the maximum slopes in the ensemble of waves, and of the slope for the aggregate ensemble.

The first two quantities are calculated from the equations

$$\alpha_r = \int_{\text{wave}} \overline{F'(\xi)^r} d\xi \quad (21)$$

$$\mathcal{M}_r = (1/\sigma_M) \int_0^{\infty} M^r P(M/\sigma_M) dM = \beta_r \sigma_M^r \quad (22)$$

We notice that α_r depends only on the shape function $F(\xi)$ that is chosen. Similarly, \mathcal{M}_r is proportional to σ_M^r but the proportionality constant β_r depends only on the statistics chosen for the maximum slope M .

The ensemble average moment, \tilde{m}_r , is related to the other two moments by the equation

$$\tilde{m}_r = \alpha_r \mathcal{M}_r \quad (23)$$

For our theory, we shall equate the value of \tilde{m}_2 , calculated from our models, to the (observable)* mean square slope σ_m^2 , so that, since

$$\beta_2 = 1,$$

$$\sigma_m^2 = \alpha_2 \sigma_M^2. \quad (24)$$

Therefore when α_2 is known, Eq. 24 relates our statistical parameter σ_M to the observable, σ_m . Values of α_2 are listed in an earlier section for most of the shape functions. If the distribution function for M contained more than one parameter then we would calculate the added parameters from other moments of the slope m than its second moment σ_m^2 .

The ensemble average fraction shadowed $\tilde{\lambda}$ can be calculated for our models from the equation

$$\tilde{\lambda}(\mu\alpha_2^{1/2}/\sigma_m) = \int_{M=\mu}^{\infty} \lambda(\mu/M)P(M/\sigma_M)d(M/\sigma_M) = \int_{\rho=\mu/\sigma_M}^{\infty} \lambda(\mu/\rho\sigma_M)P(\rho)d\rho \quad (25)$$

With exponential statistics assumed for M, the integral was evaluated analytically for all of the shape functions except Wilton's cycloid and the cosine function. Evaluation of the integral was not attempted for the cycloid because its maximum slope is fixed. Even though this condition were relaxed, its local shadowing is so similar to that for the quadratic shape function that separate calculation would not be worthwhile. For exponential statistics and the cosine shape function the ensemble average was calculated by a combination of numerical and graphical methods. For Gaussian statistics, the

*Oceanographers have determined that σ_m^2 is a linear function of the local wind speed. (See for example C. Cox and W. Munk, J. Mar. Res. 13, 198 (1954).)

function $\tilde{\lambda}$ was evaluated numerically for the Cubic A shape function and analytically for the quadratic shape function. Asymptotic formulae for large values of μ/σ_m were also developed.

The relevant analytical formulae are listed below for each shape function. It is convenient to use the quantities A and B in recording these formulae where

$$A = \alpha_2 \mu^2 / 2\sigma_m^2$$

$$B = (6\alpha_2)^{1/2} \mu / \sigma_m .$$

Quadratic

$$\tilde{\lambda} = \exp(-2^{1/2} \mu / \sigma_m) \quad (\text{Exponential})$$

$$\tilde{\lambda} = \operatorname{erfc}(A^{1/2}) + (A/\pi)^{1/2} \operatorname{Ei}(-A) \quad (\text{Gaussian})$$

where

$$A = \mu^2 / 6\sigma_m^2 .$$

For $A \gg 1$,

$$\tilde{\lambda} \sim [2(\pi A^3)^{1/2}]^{-1} e^{-A(1-5/2A + \dots)}$$

Cubic A

$$\tilde{\lambda} = (-\pi B/4) e^{-B/2} \mathcal{H}_1^{(1)}(iB/2) \quad (\text{Exponential})^*$$

where

$$B = (6/5)^{1/2} \mu / \sigma_m$$

*Dr. George Newell pointed out that the integral for this case was expressible in terms of the Bessel function $\mathcal{H}_1^{(1)}$ of an imaginary argument.

For $B \gg 1$,

$$\tilde{\lambda} \sim (\pi B/4)^{1/2} e^{-B} (1 + 3/4B + \dots)$$

$$\tilde{\lambda} = 2(A/\pi)^{1/2} \int_1^{\infty} (1-1/\xi)^{1/2} e^{-A\xi^2} d\xi \quad (\text{Gaussian})$$

where

$$A = 3\mu^2/5\sigma_m^2$$

For $A \gg 1$,

$$\tilde{\lambda} \sim (1/2)^{3/2} A e^{-A} (1 - 21/16A + \dots)$$

Cubic B

$$\tilde{\lambda} = e^{-B} - (\pi B/4)^{1/2} \operatorname{erfc} B^{1/2} \quad (\text{Exponential})$$

where

$$B = (2/5)^{1/2} (\mu/\sigma_m)$$

For $B \gg 1$,

$$\tilde{\lambda} \sim (1/2) e^{-B} (1 + 1/2 B + \dots)$$

6. "Lower Limit" of the Fraction Shadowed

We have already seen that the fraction of surface with slope greater than μ should be less, for any one of the shape functions of the first model, than the fraction of the surface that is shadowed, and thus that $\tilde{\lambda}_*$ should be a lower limit for $\tilde{\lambda}$. Since $\tilde{\lambda}_*$ is more easily calculated from observational data than is $\tilde{\lambda}$, we can calculate the former for a second and less restricted model of a rough surface than the model used so far and in this way find the range of validity of the calculations of $\tilde{\lambda}$.

All that is needed to calculate $\tilde{\lambda}_*$ is the distribution function of slopes on the surface, which was shown by Cox and Munk (loc. cit.)

to be approximated well by a Gaussian function. The chance that a slope is larger than μ is then

$$\tilde{\lambda}_{*0} = \text{erfc}(\mu / \sqrt{2} \sigma_m) \quad (26)$$

where we have added the subscript zero to identify this particular calculation of $\tilde{\lambda}_*$. This ensemble fraction shadowed is the same as for a saw tooth surface, for which $\lambda_* = 1$ for $0 \leq v \leq 1$, with Gaussian statistics of the slope M .

In arguing that this is a supposed lower limit to the fraction shadowed $\tilde{\lambda}$, we have not only used assumptions a) and b) listed earlier but also have ignored the correlation between adjacent waves. We have also assumed that the chance that an observed slope will be larger than μ is equal to the fractional area of the sea surface that has slope greater than μ .

7. Discussion

The average fractions shadowed $\tilde{\lambda}$ of the wave ensemble, computed from the formulae in the preceding sections for the first model, are plotted as functions of (μ/σ_m) in Fig. 6, together with the curve for the supposed "lower limit" $\tilde{\lambda}_{*0}$ of the second model. For the first model, only the curves for exponential statistics are shown because the substitution of Gaussian for exponential statistics, used with the quadratic and cubic A shape functions, was found to change the calculated values of $\tilde{\lambda}$ by less than 10%. The behavior of $\tilde{\lambda}$ for large (μ/σ_m) is what we should expect from the asymptotic formulae given previously. From Fig. 6 we can also see that the choice of the shape function affects the value of $\tilde{\lambda}$ markedly except when (μ/σ_m) is about equal to 1.5 and $\tilde{\lambda}$ is about equal to 0.2.

The $\tilde{\lambda}$ curves for the quadratic and cosine shape functions appear to be reasonable since they lie somewhat above the lower limit curve for

large values of (μ/σ_m) . Both shape functions are also realistic rough approximations to waves at sea under different conditions. There is the advantage in using the quadratic shape function that all calculations are much simpler than for the cosine function.

The ensemble shadowing curves for Cubics A and B are quite different than the curves for the other shape functions. It is clear from comparison of the curves in Fig. 6 that the ensemble average fraction shadowed is less for an asymmetric than for a symmetric wave if the sharp crest is farther from the source than is the smooth crest of the wave. The opposite is true if the positions of the smooth and sharp crest are interchanged. On the basis of what we have investigated we cannot say whether the different shadowing can be ascribed partly to the asymmetrical slopes of the cubic shapes or to the asymmetrical curvatures of the right and left hand crests. Comparison of observed and calculated moments of the surface slope would illuminate this question, for then we could find what added restrictions should be placed upon the shape function $\square(\xi)$ and the distribution function $(1/\sigma_M)P(\mu/\sigma_M)$. It would probably then be discovered that cubics A and B represent such extremes of asymmetry as to preclude their use as shape functions for individual waves of an ensemble of real wind waves. We suspect also that our statistics for Cubic A are wrong because even for very large values of (μ/σ_m) , where Cubic A should lead to an accurate approximation to the shadowing of any smooth-crested wave, the Cubic A curve lies below the lower limit curve.

From Fig. 5 we should have expected that the curve for the lower limit $\tilde{\lambda}_{*0}$ would have been lower than any of the other curves by a factor

lying between $1/3$ and 1 . We observe that this is true only (excepting the Cubic A curve) when the value of (μ/σ_m) is greater than one or two. The fraction shadowed, for this value of the abscissa, is of the order of 0.1 or 0.2 . We may say then that for larger fractions shadowed our calculations based on the first model presumably are not realistic. Even without reference to the lower limit curve of the second model we know that for small enough grazing angles or large enough fractions shadowed the first model will become unrealistic because of the neglect of the shadowing of one wave by neighboring waves. Although the reason for the discrepancy between the curves for the first and second models is not at present known, it is encouraging that agreement for all but Cubic A between the results for the two models is found in the same region of large grazing angles for which the assumption of equal crest heights in the first model should be valid.

We may add that neither the first nor the second model takes into account the ordering or arrangement of the individual waves. The second model also implies nothing about the ordering of the slopes of the waves.

It would be possible to improve the calculation of $\tilde{\lambda}$ for the first model and for large values of the grazing angle by methods previously indicated if the statistics of maximum slope of the surface were known so that Cubic A, which has been shown to be accurately representative locally, could be used as the proper shape function. It would also be possible to elaborate both the first and second models and the statistics so that more than one crest was included between the two high and equal neighboring crests defining what we have called a single resultant wave.

The low angle case however is the more important for comparison with experiments, and is not easily approachable by such elaborations

of the next model. It is thus more useful to study first this low angle case in which the crests cannot be assumed to be of equal height and the randomly placed, infrequent, high crests are the only parts of the surface which produce shadowing. A discussion of this low angle problem is given in Part II.

PART II. THEORY FOR SMALL GRAZING ANGLES

8. Development of the Theory

A third model is appropriate to use in calculating the shadowing when the grazing angle relative to the plane of mean sea level (MSL) of the incident ray is very small. Consider that a line source of radiation exists which directs a beam of slope $\mu \ll 1$ toward the rough surface. (See Fig. 7.) Let the elevation of the source above MSL be z_0 where z_0 is larger than the height of almost any wave. Let the line source be parallel to the y axis and be of linear width Δy and angular width $\Delta\theta = \Delta\mu$ in elevation. Let L_x and L_y be the mean wave lengths of the rough surface in the x and y directions. Finally, suppose that $\Delta y = nL_y$ where $n \gg 1$ so that the beam cuts out a patch on the surface that is much wider than one wave-length.

As energy in the beam approaches the rough surface, power is lost from it because sections of the beam occasionally encounter the higher parts of the waves. We assume that this blocking action can be described by a coefficient $\xi(z)$, the attenuation per unit length of slant range R. We suppose that $\xi(z)$ depends only upon z and not upon μ . Its interpretation will be given later.

If the beam contains power in the amount $S\Delta y\Delta\mu$ at height z then this density function $S(z)$ changes along the beam according to the relation

$$-dS = S\xi dR. \quad (27)$$

In this direction $dR = -dz/\mu$. Therefore, if $S_o = S(z_o)$,

$$S(z) \Delta y \Delta \mu = S_o \Delta y \Delta \mu \exp \left[-\mu^{-1} \int_z^{z_o} \xi(z) dz \right]. \quad (28)$$

This is the power illuminating the flat patch of area ΔA_s cut out from any horizontal plane at height z by the wedge beam. For $z = 0$ (MSL), this flat patch has an area $\Delta A_s = -\Delta y (\Delta \mu / \mu) R$ and is the projection of the area dA_r cut out of the rough surface by the beam. We assume that the illumination of dA_r is larger by a factor $\mathcal{D}(\mu)$ than that of dA_s where \mathcal{D} is a weak function of μ . Then the power illuminating the rough patch of surface dA_r is

$$\mathcal{D}(\mu) S(o) \Delta y \Delta \mu \quad (29)$$

whereas if there had been no shadowing of this area, it would have been illuminated by a power

$$\mathcal{D}(\mu) S_o \Delta y \Delta \mu \quad (30)$$

The fraction of that area that is illuminated, therefore, is $S(o)/S_o$ which is also equal to the fraction of the surface that is unshadowed, $(1 - \tilde{\lambda})$. Consequently

$$\tilde{\lambda} = 1 - \exp \left[-\mu^{-1} \int_0^{z_o} \xi(z) dz \right] \quad (31)$$

The integral of $\xi(z)$ can be given a qualitative interpretation in terms of parameters describing the surface roughness.* Let us consider the wedge of width nL_y and angular aperture $d\mu$ (Fig. 8), and its intersection with parts of the water surface at height z and lying in a band

*This interpretation must be modified if the curvature of the earth is taken into account.

of length L_x in the x direction. The areas cut out will extend the length $dz = R d\mu$ in the z direction. In particular, consider the projection on the y - z plane of the crests in the band and of the areas of water cut out, on the source side of these n crests, by the wedge of radiation. On the average there will be about n non-overlapping projections of the crests that lie in the band. Two of these projected areas are sketched in Fig. 8. The length in the y direction of the area cut out from i-th crest in the band we call y_i . Then the total area blocking passage of radiation

through the band is $\sum_{i=1}^n y_i dz$. The fraction of the wedge area at height z that is thus blocked is

$$\sum_{i=1}^n y_i / nL_y = \bar{y}(z) / L_y \quad (32)$$

where $\bar{y}(z)$ is the average projected width of the waves at height z in the band $nL_y \cdot L_x$.

Now consider a longer block $mL_x \cdot nL_y$, where $mL = \Delta R$ and $m \gg 1$. The fraction of the wedge blocked now is

$$A_1(z) \left[\bar{y}(z) / L_y \right] (\Delta R / L_x) \quad (33)$$

where we have added the factor $A_1(z)$ to allow for the fact that projections of waves lying in successive L intervals may overlap. For the case we are considering, that is for $\mu \ll 1$, $\xi(z)$ will not change rapidly over the increment of range ΔR . We can thus identify the coefficient of ΔR in the above expression as $\xi(z)$,

$$\xi(z) = A_1(z) \bar{y}(z) / L_x L_y \quad (34)$$

Then

$$\begin{aligned} \int_0^{z_0} \xi(z) dz &= (L_x L_y)^{-1} \int_0^{z_0} \Lambda_1(z) \bar{y}(z) dz \\ &= (\bar{\Lambda}_1 / L_x L_y) \int_0^{z_0} \bar{y}(z) dz \end{aligned} \quad (35)$$

where $\bar{\Lambda}_1$ is a mean value of $\Lambda_1(z)$. Using the fact that z_0 is higher than almost any wave we see that

$$\int_0^{z_0} \xi(z) dz = (\bar{\Lambda}_1 / L_x) \bar{h} \quad (36)$$

where \bar{h} is the mean height above mean sea level of the projected wave profile. The ratio (\bar{h}/L_x) can be taken proportional to the wave steepness $\delta = H/L_x$. For models which assume that the smaller waves are smoothed out, we can also say that this ratio is proportional to the rms wave slope σ_m in the x direction,

$$\bar{h}/L = \Lambda_2 \sigma_m \quad (37)$$

so that finally

$$\int_0^{z_0} \xi(z) dz = \Lambda \sigma_m \quad (38)$$

where $\Lambda = \bar{\Lambda}_1 \Lambda_2$. We have thus found that the integral of the attenuation coefficient $\xi(z)$ should be proportional to σ_m , the rms wave slope.

Our final expression for the fraction shadowed, for small grazing angles, of the strip ($nL_y \Delta R$) is then

$$\tilde{\lambda} = 1 - \exp(-\Lambda \sigma_m / \mu) \quad (39)$$

This variation of $\tilde{\lambda}$ with μ is extremely rapid for small μ . In fact,

$\tilde{\lambda}$ is essentially constant over a small range $\Delta\mu = \Delta\mu_1$ of μ only if

$(\Delta\mu_1 \Delta\sigma_m / \mu^2)$ is small compared to one. Experimental measurements will generally be concerned with the average of the fraction shadowed over a finite range of μ that is larger than $\Delta\mu_1$.

9. Discussion

It appears to be reasonable to assume that the form of the relationship between $\tilde{\lambda}$ and (μ/σ_m) is correct in the low angle case if other sea state parameters than the rms wave slope are ignored. In order, however, to choose a reasonable value for the parameter we at present must depend upon qualitative arguments. Let us first compare the predictions of Eq. 39 with those of the second model. Values of $\tilde{\lambda}$ from Eq. 39 are plotted in Fig. 9 for $\Lambda = 0.3, 0.6, \text{ and } 1.0$. For (μ/σ_m) less than one we note that Λ must be greater than about 0.5 if the lower limit curve of model two is not to lie above a low angle curve from Eq. 39. We conclude, therefore, that Λ cannot be less than about 0.5. This conclusion is conservative because our earlier discussion shows that the lower limit curve is low by a substantial amount in the small angle region.

We next inquire as to what values of $\Lambda = \bar{\Lambda}_1 \Lambda_2$ correspond to specific wave shapes. Consider first the second factor, Λ_2 , whose value can be calculated for any given wave shape. For the quadratic and cosine wave shapes, for example, we find the values 0.29 and 0.16 respectively. The first factor $\bar{\Lambda}_1$ can, from its definition, not have a value greater than one. The product Λ would then, for the two wave shapes cited, have a value less than 0.3, resulting in a fraction shadowed that is less than that given by the lower limit, for most values of (μ/σ_m) .

Remembering that the estimates of Λ_2 are based on wave shapes that are not very realistic for the low angle case and that Λ must be somewhat larger than 0.5 in order to avoid crossing the lower limit curve, we propose that a value of 0.6 be assumed for Λ for low angle shadowing.

We estimate finally a single shadowing curve for all grazing angles. We know that the second model involves no unknown parameters but yields values of the fraction shadowed which may be low, according to Fig. 5, by 30-50 %, for large grazing angles. For such angles it is thus appropriate to use the shadowing curve based upon the first model. We use the quadratic shape function for the rather weak reasons given in Part I. For small grazing angles the third model gives us the best approximation. An estimated curve for grazing angles from small to large can then be obtained by fairing in a curve which approaches the 0.6 curve for small angles and the quadratic curve for large angles. This curve is marked with crosses in Fig. 9.

CONCLUDING REMARKS

Our calculations make it reasonable to assume that the fraction shadowed is, in first approximation, dependent only upon the ratio (μ/σ_m) of the slope μ of the incident ray and the rms slope σ_m of the waves for all grazing angles. The functional form of the dependence was determined for a number of special models, and these forms may be useful in correlating experimental data. The theory is incomplete because it contains no good estimate of the validity of the models and because surface roughness (or sea state) parameters other than the rms wave slope are ignored.

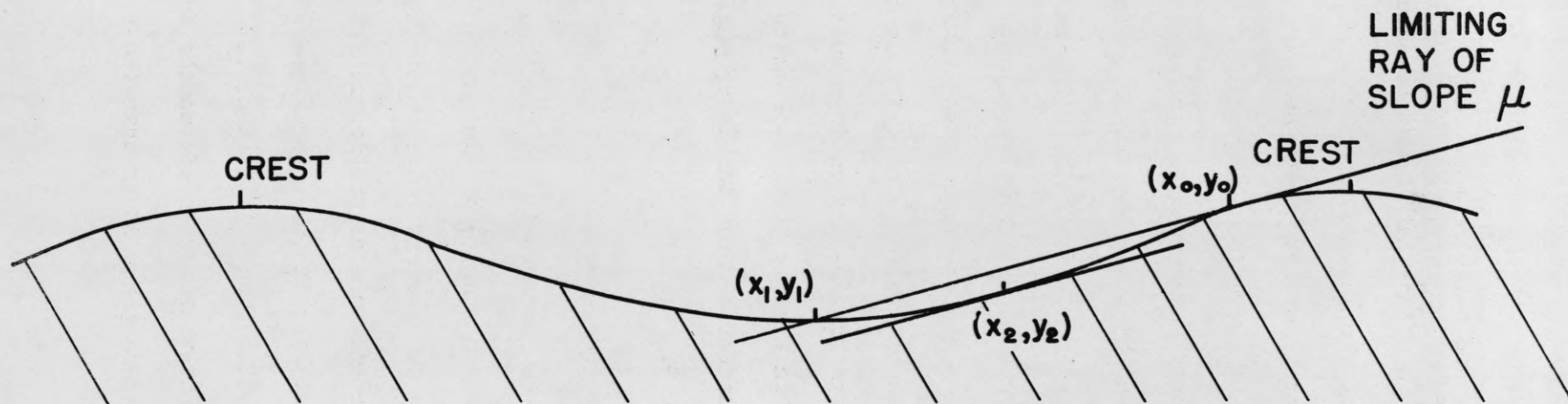


FIG. I.
A LIMITING RAY

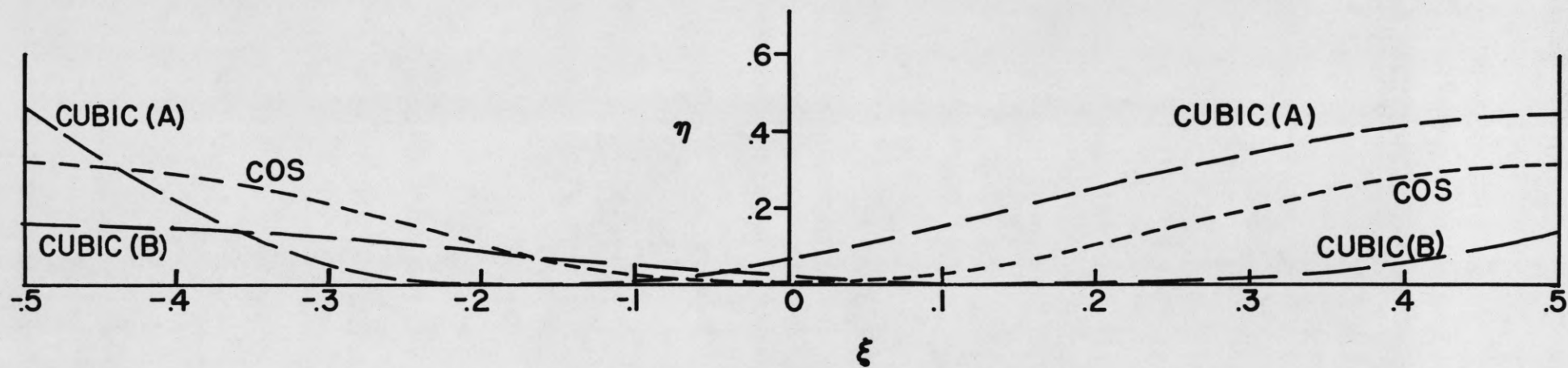
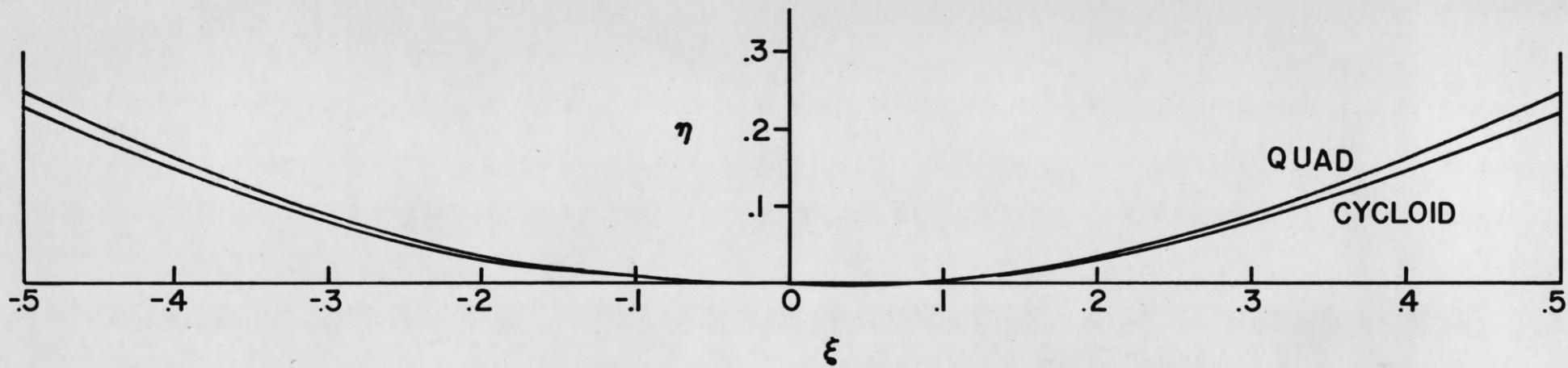


FIG. 2.
SHAPE FUNCTIONS

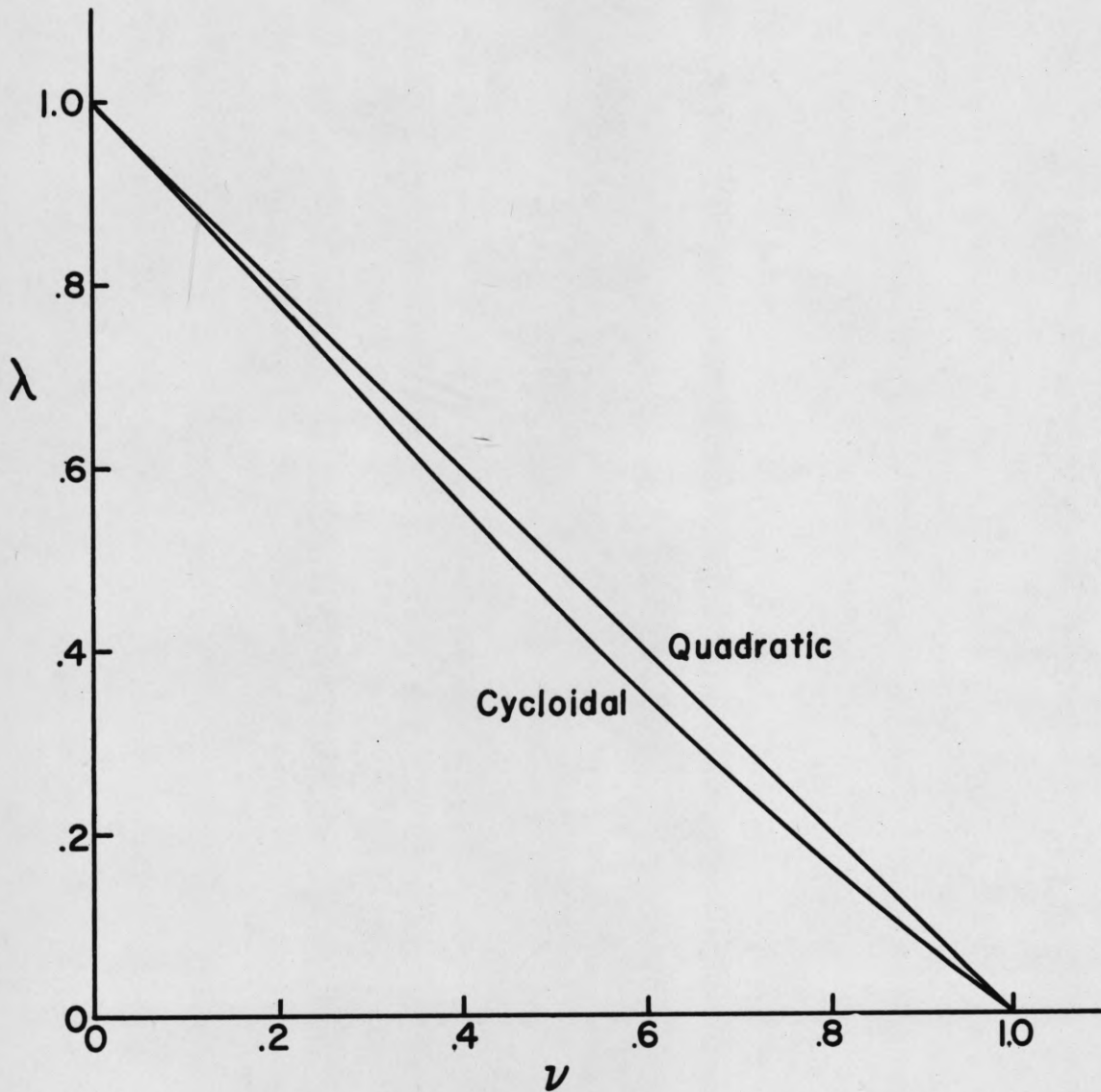


FIG. 3.
LOCAL SHADOWING-TWO SHARP CRESTS

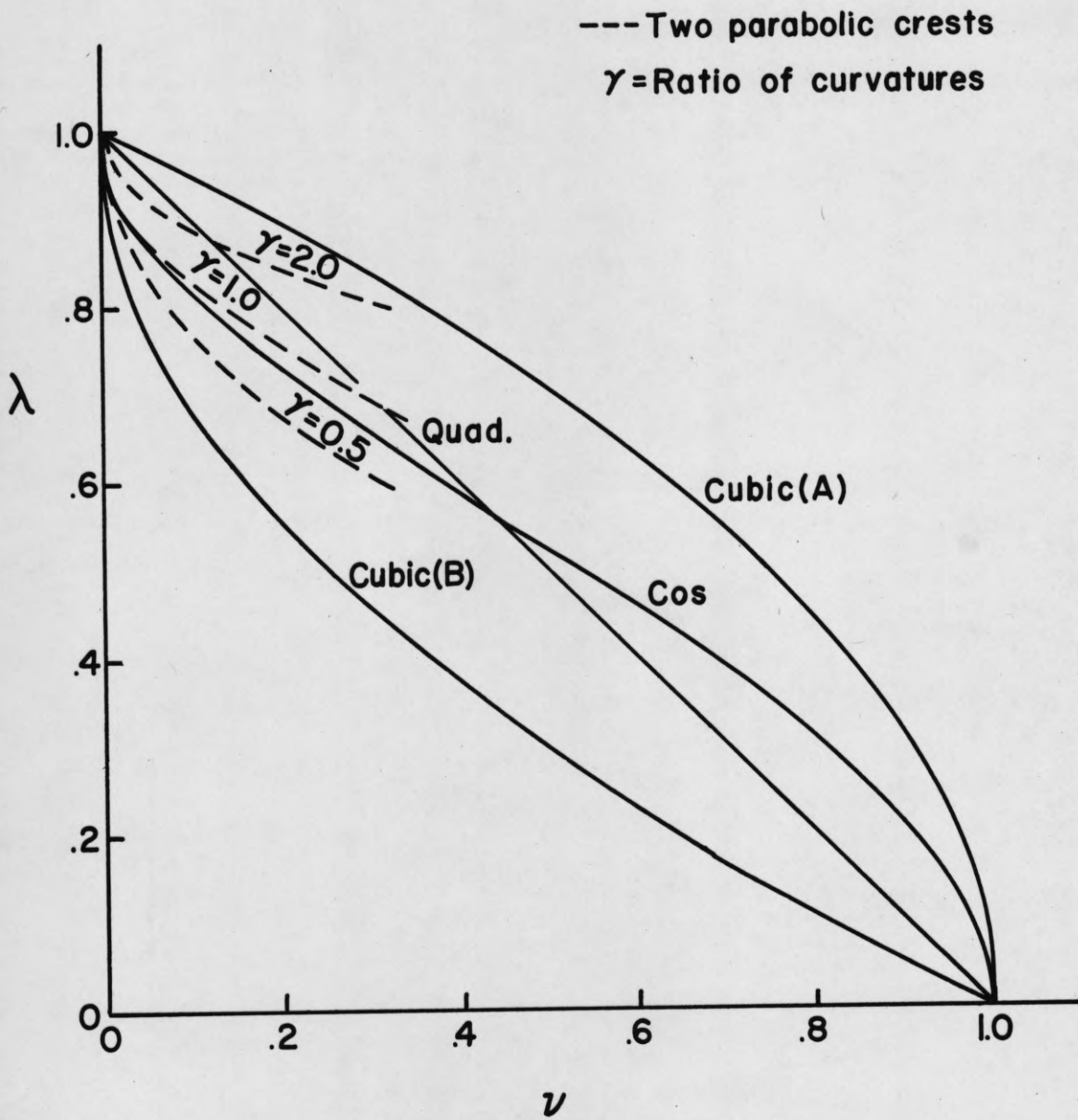


FIG. 4.

LOCAL SHADOWING-ONE OR TWO SMOOTH CRESTS

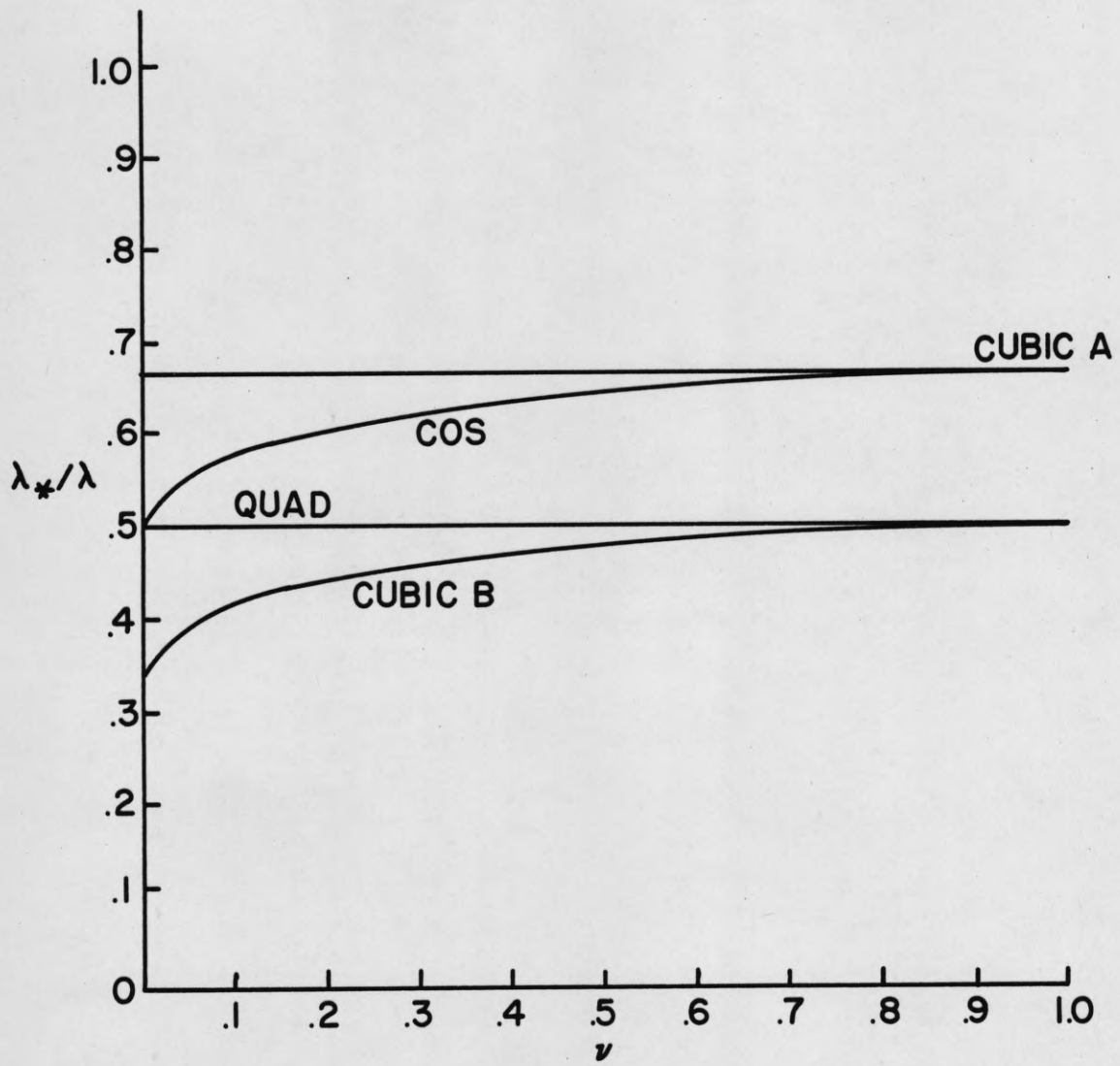


FIG.5.

LOCAL SHADOWING-COMPARISON OF TWO ESTIMATES

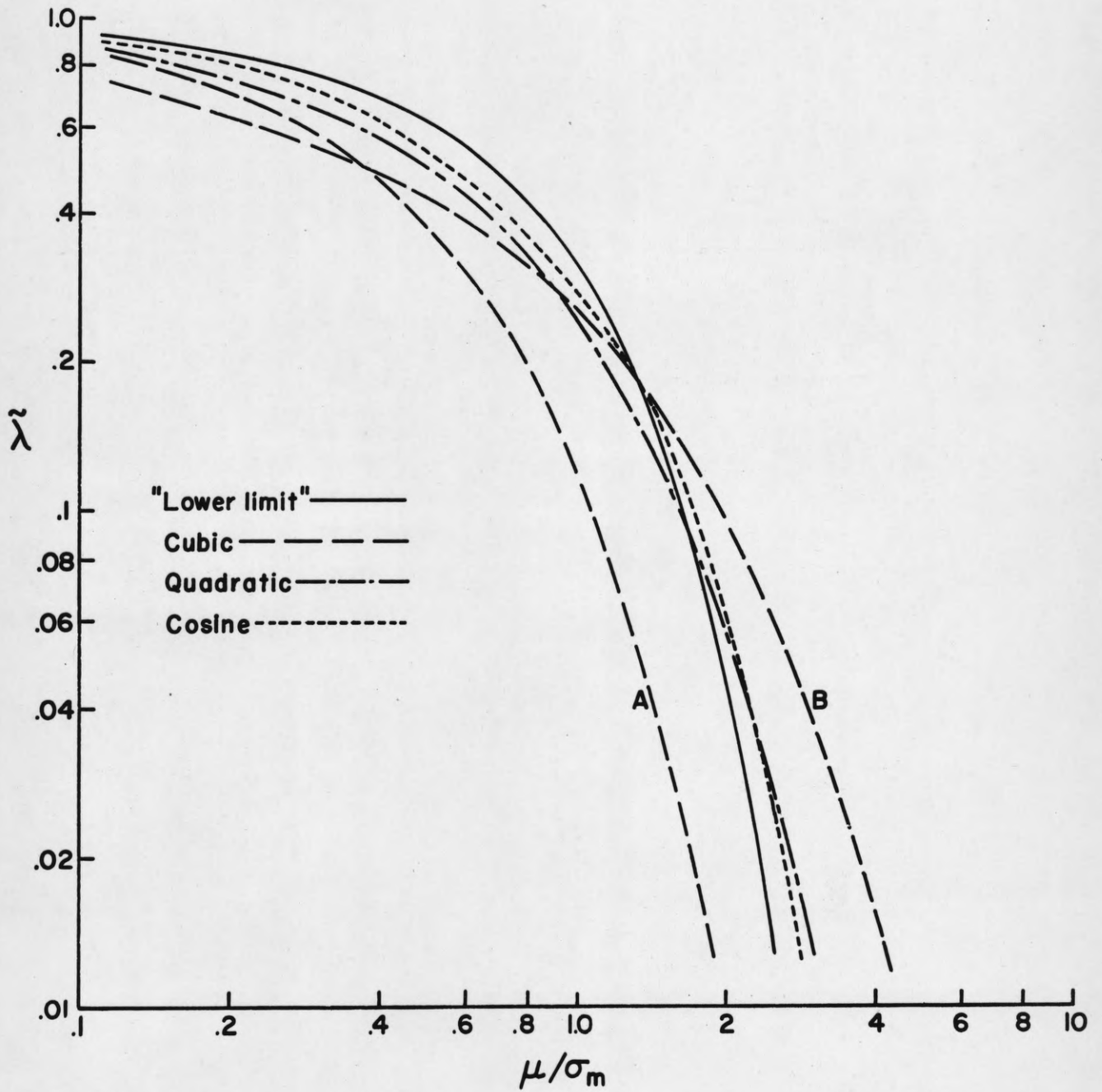


FIG. 6.
ENSEMBLE SHADOWING- VALID FOR LARGE μ/σ_m

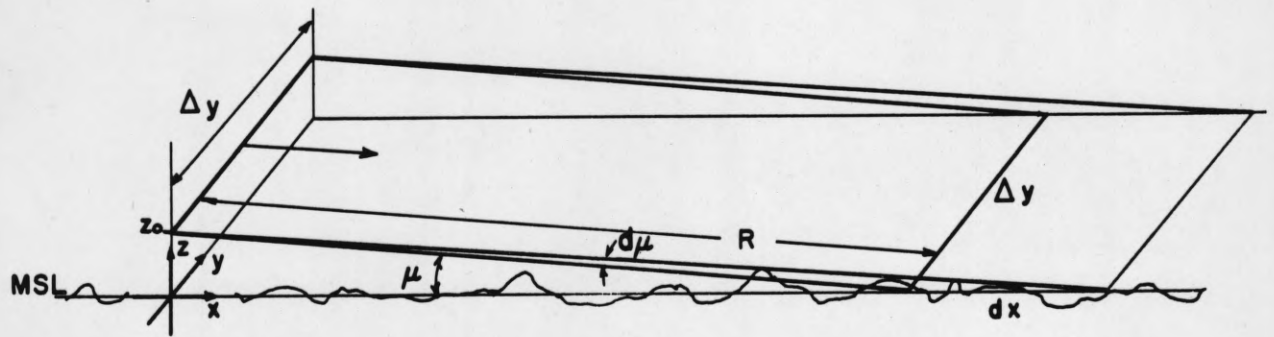


FIG. 7. LOW ANGLE SHADOWING

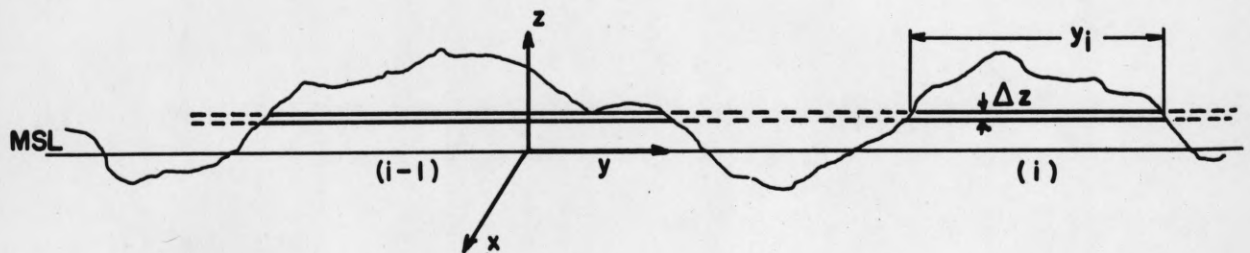


FIG. 8. PROJECTION OF WAVES ON yz PLANE

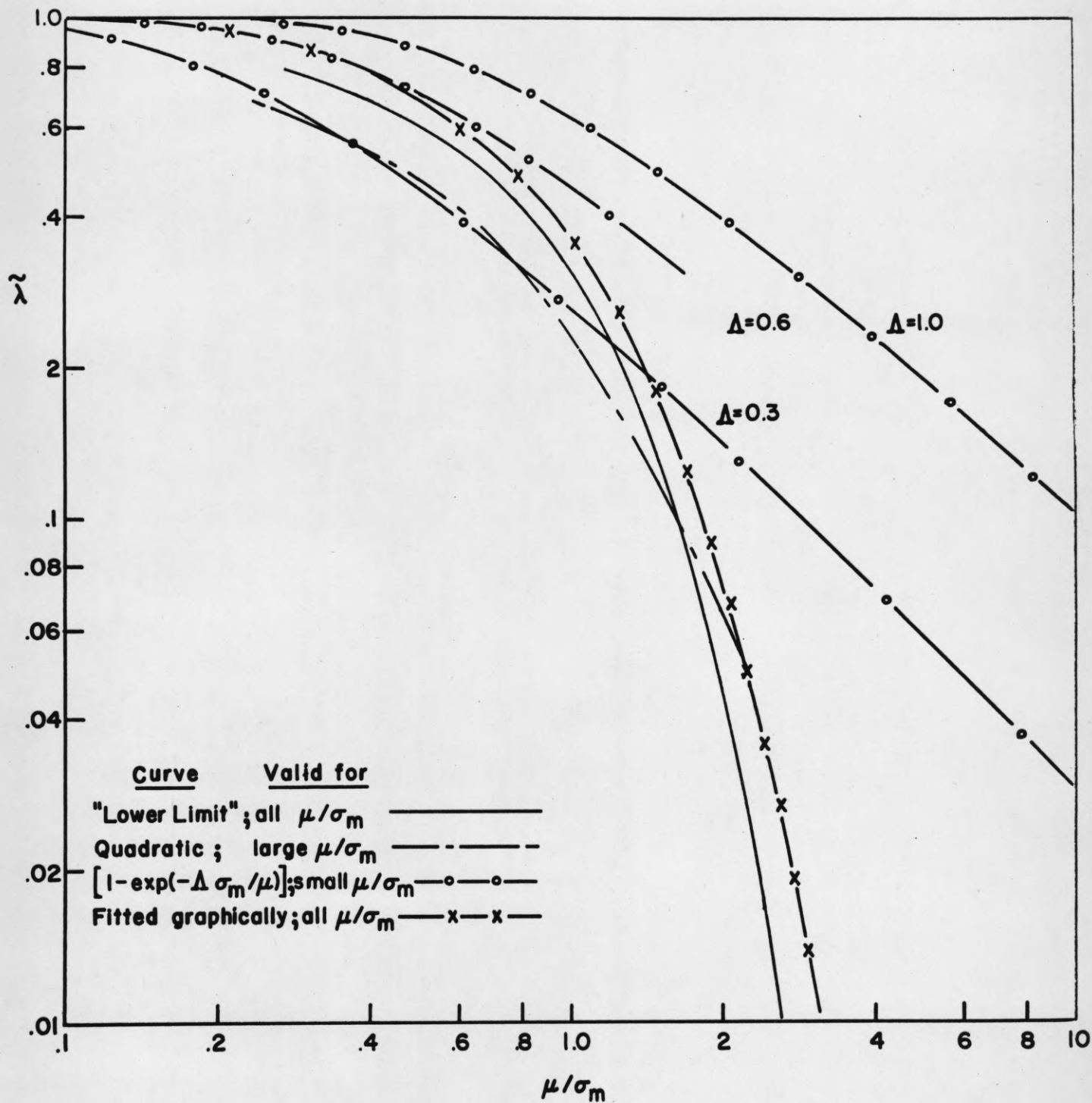


FIG. 9. ENSEMBLE SHADOWING-APPROXIMATIONS FOR VARIOUS RANGES OF μ/σ_m